Journal of the Korean Nuclear Society
Volume 33, Number 4, pp.370~381, August, 2002

Neutron Cross Section Evaluation on Pr-141, Nd-143, Nd-145, Sm-147 and Sm-149

Y. D. Lee and J. H. Chang
Korea Atomic Energy Research Institute
150 Dukjin-dong, Yuseung-gu, Daejon 305-353, Korea
ydlee@kaeri.re.kr

(Received February 5, 2002)

Abstract

The neutron induced nuclear data for Pr-141, Nd-143, Nd-145, Sm-147 and Sm-149 were calculated and evaluated from 10 keV to 20 MeV. The energy dependent optical model potential parameters were extracted based on the recent experimental data and applied up to 20 MeV. The s-wave strength function was calculated. Spherical optical model, statistical model in equilibrium energy, multistep direct and multistep compound model in pre-equilibrium energy and direct capture model were introduced in Empire calculation. The theoretically calculated cross sections were compared with the experimental data and the evaluated files. The model calculated total and capture cross sections were in good agreement with the reference experimental data. The capture cross sections in pre-equilibrium were enhanced in recent released Empire version. The evaluated cross section results were compiled to ENDF-6 format and will improve the ENDF/B-VI.

Key Words : neutron, cross section, evaluation, fission products

1. Introduction

The priori fission products[1] were selected for the neutron cross section evaluation, which mainly influence on reactivity in a fission reactor. The evaluation for the selected fission products has been jointly performed with National Nuclear Data Center (NNDC) of Brookhaven National Laboratory (BNL). The evaluation is divided into two regions: resonance region[2] and upper resonance region up to 20 MeV. Different theory and procedure are applied in each energy region for cross section production and evaluation. In this paper, the cross section calculation and evaluation were performed only for latter energy region. The results of two regions will be merged to make full neutron data set.

Neutron induced nuclear reaction data for fission products are important for several applications: prediction of burnup performance in a fission reactor, criticality calculation for spent fuel storage design, advanced fuel performance analysis and radiation damage estimation of structural material. Specially, neutron capture cross section of the selected fission products is considerable cross section concerning neutron absorption loss.

Sm-147 and Sm-149 have a high yield and long lifetime in a reactor. They are mainly accumulated from beta decay and electron capture from precursors. Pr-141, Nd-143 and Nd-145 are stable isotopes. They are also accumulated by beta decay, electron capture or alpha decay in a reactor. Neodymium isotopes are important material in waste storage concerning decay heat. In ENDF/B-VI, the evaluation on Pr-141, Nd-143 and Nd-145, Sm-147 and Sm-149 were done at 1980, 1992, 1989 and 1978, respectively. Therefore, a new evaluation with better theory is required based on the recent experimental data for better application.

The evaluation consists of an optical model potential search followed by a complete nuclear reaction model calculation and validation to the experimental data. The optical model potential depending on the incident neutron energy is searched using recently developed graphical interface[3] to the ABAREX[4]. Potential form and corresponding parameters are selected and decided by comparing the model calculated total and elastic scattering cross sections with the reference experimental data. The s-wave strength function by the extracted potential parameters is compared with that of the evaluated in the resonance region.

Nuclear reaction cross sections were calculated by using the recently released Empire-II code[5]. This code consists of several modules: optical model, Hauser-Feshbach model in equilibrium calculation and quantumn mechanical approach in pre-equilibrium calculation. The width fluctuation correction in Hauser-Feshbach influenced on the capture and inelastic scattering cross sections. The code offers several built-in libraries including the ENSDF nuclear level and decay schemes, nuclear masses, ground state deformations and γ-ray strength functions. The calculated cross sections are graphically compared with the experimental data and the evaluated files (ENDF/B-VI, JENDL-3.2, JEF-2.2, BROND-2 and CENDL-2). The evaluated results are compiled to ENDF-6 format and experience its physics check.

2. Model Theory

2.1. Optical Model Potential

Available published optical model potentials are limited in the incident neutron energy, target A or Z range. Reference Input Parameter Library (RIPL) published by IAEA involves several different optical model potential shapes and corresponding parameters for many nuclides and incident neutron energies. For the selected fission products, the possible potential in RIPL[6] is very restricted and even, the potential does not reproduce the total and elastic scattering cross section properly to the recent experimental data.

The potential form and corresponding parameters, as a function of incident neutron energy, were searched in a spherical optical model[4] based on the reference experimental data. To obtain proper potential parameters, the Woods-Saxon well is used for the real part potential in optical model:

$$V(r) = -V/(1+\exp((r-R_v)/a_v)) \quad (1)$$

where V and a_v are the strength and diffuseness of the potential. The nuclear radius R_v, related to mass number A, is given by

$$R_v = r_v A^{1/3}. \quad (2)$$

For the imaginary part potential, the derivative Woods-Saxon shape is used,

$$W(r) = -4W\exp((r-R_w)/a_w) / (1+ \exp(r-R_w)/a_w)^2 \quad (3)$$

where W, R_w and a_w are potential strength, radius

and diffuseness, respectively. Generally, Thomas form is taken in the optical model potential for spin-orbit coupling:

$$V_{s\text{-}o}(r) = (2L \cdot S)V_{so}(2/r)d/dr(1/[1+\exp((r-R_{so})/a_{so})]) \quad (4)$$

where $L \cdot S$ is the dot product of the orbital and spin angular momentum operator.

The real and imaginary potential strength and radius are expanded as a function of incident neutron energy:

$$V = V_o + V_1 E_n,\ r_v = r_o + r_1 E_n, \quad (5a)$$

$$W = W_o + W_1 E_n,\ r_w = r_{wo} + r_{w1} E_n, \quad (5b)$$

where E_n is an incident neutron energy. The potential parameters in JENDL[7] were used as an initial value for searching process. JENDL does not have energy dependence in radius. JENDL potential needed a tuning to get better cross sections to the recent experimental data. Moreover, the s-wave strength function value produced by JENDL potential was different from the reference value[2] evaluated in the resonance region. Potential parameters can be used in the region of interesting energy range. However, the potential parameters (V_o, V_1, W_o, W_1, r_o, r_1, r_{wo}, r_{w1}, a_v, a_w, V_{so}, r_{so}, a_{so}) were searched from 1 keV to 20 MeV.

ABRXPL displays the calculated total and capture cross sections, angular and energy dependent elastic scattering cross sections and energy dependent potential shape in different option. This enables user to obtain the optical model potential parameters for a given nucleus over the whole energy region of interest. ABRXPL creates ABAREX input file and runs ABAREX. ABRXPL can also be used as a powerful tool to understand the cross section change by different optical model potential form or parameters. The procedure for optimized optical model potential parameters is followed:

1. Select reference total, elastic scattering and capture cross sections
2. Prepare input for ABAREX run: target nucleus information (A and Z number, level energy, spin, parity, spin cut-off, temperature, binding energy, level density parameter, giant dipole energy), energy range, energy dependent potential form, initial value for potential parameters
3. Run ABAREX through ABRXPL
4. Display the extracted cross sections and s- and p-wave strength function value with reference experimental data on the screen
5. Determine potential parameters interactively by eye-guide decision
6. If not satisfied, change potential parameters and go to 3.

The potential parameters will be used for the next process of nuclear reaction cross section generation process. The potential produces total, elastic scattering and reaction cross sections, s-(So) and p-wave strength function (S_1) values and transmission coefficients as well as scattering radius.

Many fission products have their first excited level energy at several tens of keV or higher. As a reference energy for So, 1 keV was selected as a lower bound energy in the unresolved region to compare the So calculated from the selected potential with that evaluated by the recent resonance parameters at resonance region. For some fission products, the experimental data for total and elastic scattering cross sections are not available. In these cases, So evaluated in the resonance region is a crucial reference in optical model potential parameter searching.

2.2. Reaction Cross Section

Empire-II was used to compute the reaction cross sections with transmission coefficients obtained from the optical model. Empire accounts for the major nuclear reaction mechanisms, such as Multistep Direct (MSD), Multistep Compound (MSC) and the full featured Hauser-Feshbach model. The Hauser-Feshbach decay for particles and gamma rays with the width fluctuation corrections was introduced into the calculation of cross sections. The cross section in Hauser-Feshbach theory between the incident and outgoing waves in the decay channels is defined by

$$\sigma^{HF} = \pi \lambda_a^2 T_\alpha T_\beta W_{\alpha\beta} / \sum_i T_i, \qquad (6)$$

where $W_{\alpha\beta}$ is the width fluctuation correction factor. This factor depends on the transmission coefficients (T_i). T_α and T_β are the transmission coefficients of a reaction channel α and a decay channel β. Recently, direct capture model was inserted into Empire to enhance the capture cross section in pre-equilibrium energy region. The model assumes that γ emission occurs through the de-excitation of the Giant Dipole Resonance (GDR).

The Multistep direct model takes care of the inelastic scattering to vibrational collective levels and decay information. In Multistep Direct approach, continuum scattering is considered as a sequence of 1p-1h transitions and the transition strength functions correspond to response functions of an external one-body operator acting repeatedly on a nucleus. The approach to statistical multistep direct reaction is based on the Multistep Direct theory of pre-equilibrium scattering to the continuum originally proposed by Tamura, Udagawa and Lenske[8]. The modeling of Multistep Compound processes follows the approach of Nishioka et at. (NVWY)[9]. Like most of the pre-compound models, the NVWY theory describes the equilibration of the composite nucleus as a series of transitions along the chain of classes of closed channels of increasing complexity.

3. Evaluation

Table 1 shows the used reference experimental data and the 1st excited energy for each isotope. The upper energy of the unresolved resonance region was set to the energy where the 1st inelastic scattering reaction channel opens. The searched potential parameters are summarized in Table 2. The potential depth for the real and imaginary has the range from 46 MeV to 52 MeV and from 6 MeV to 9 MeV. The radius varies from 1.2 fm to 1.28 fm for the real and from 1.18 fm to 1.27 fm

Table 1. Reference Experimental Data and 1st Excited Energy

Isotope	Reference experimental data		1st excited energy
	Total cross section	(n, γ) cross section	
Pr-141	Singh[10], Kellie[11] and Foster[12]	Zaikin[13]	145 keV
Nd-143	Wisshak[15]	Wisshak[15]	742 keV
Nd-145	Wisshak[15]	Wisshak[15]	67 keV
Sm-147	Wisshak[16]	Wisshak[16]	121 keV
Sm-149	Wisshak[16]	Wisshak[16]	23 keV

Table 2. Potential Parameters as a Function of Incident Neutron Energy

Parameter (unit)	Pr-141	Nd-143	Nd-145	Sm-147	Sm-149
V_o(MeV)	46.00	46.6600	48.7900	52.1870	52.6878
V_1(MeV)	-0.2000	-0.2000	-0.2000	-0.0330	-0.0330
r_o(fm)	1.2866	1.2639	1.2526	1.2450	1.2220
a_v(fm)	0.560	0.638	0.580	0.739	0.635
W_o(MeV)	5.800	7.490	6.330	7.670	9.130
r_{wo}(fm)	1.2750	1.1852	1.2500	1.2420	1.2200
a_w(fm)	0.460	0.614	0.536	0.568	0.590
V_{so}(MeV)	7.000	7.000	7.000	9.600	8.200
r_{so}(fm)	1.275	1.280	1.280	1.231	1.231
a_{so}(fm)	0.620	0.600	0.600	0.683	0.683
W_1(MeV)	0.300	0.000	0.000	-0.102	-0.102
r_{w1}(fm)	0.000	0.000	0.000	0.000	0.000
r_i(fm)	0.000	0.000	0.000	-0.010	-0.010

Table 3. Comparison of s-wave Strength Function

Isotopes	s-wave strength function	
	In ABAREX	By evaluation*
Pr-141	1.930E-4	1.770E-4
Nd-143	3.303E-4	3.620E-4
Nd-145	4.000E-4	4.750E-4
Sm-147	5.020E-4	4.860E-4
Sm-149	4.689E-4	4.530E-4

* from the resonance parameters[2]

for the imaginary part. The potential depth for real part was not changed significantly in neodymium and samarium isotopes. However, the difference between neodymium and samarium was shown. The radius for real and imaginary part was not varied much in the isotopes. The imaginary potential depth was varied in each isotope. The potential for spin-orbit coupling did not give much influence on neutron cross section data generation.

The s-wave strength function (S_o) was calculated at 1 keV in the optical model, by the searched potential parameters. From Table 3, the calculated S_o values are close to those by the recently evaluated resonance parameters in the unresolved resonance energy region. Therefore, the S_o will help to merge smoothly the evaluation results of the different energy regions with the different models in the unresolved energy region.

All input parameters for Empire were prepared and the tuning of parameters was necessary. The cross sections are calculated on (n, tot), (n, n), (n, n'), (n, 2n), (n, 3n), (n, nα), (n, np), (n, γ), (n, p) and (n, γ) from 10 keV to 20 MeV[22]. The calculated cross sections are graphically compared with the experimental data and the evaluated files for all reaction channels. In this paper, (n, tot), (n, n'), (n, γ), (n, p) and (n, α) cross sections are introduced with the experimental data and the evaluated files.

Fig. 1 shows the comparison of the calculated result to the experimental data[10,11,12] and ENDF/B-VI for total cross section of Pr-141. The model calculated total cross section by the searched optical model potential was in good agreement with the experimental data. However, the calculation is somewhat lower than ENDF/B-VI. Specially, below 300 keV, the deviation starts bigger. At low energy, the s-wave strength

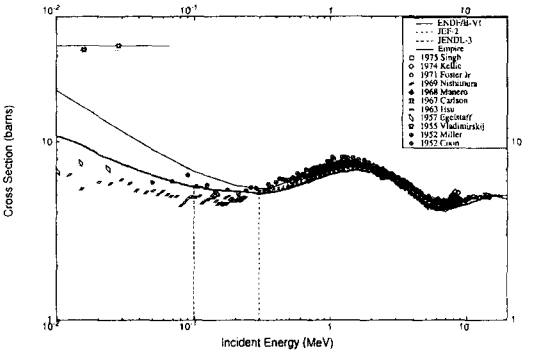

Fig. 1. Total Cross Section for Pr-141

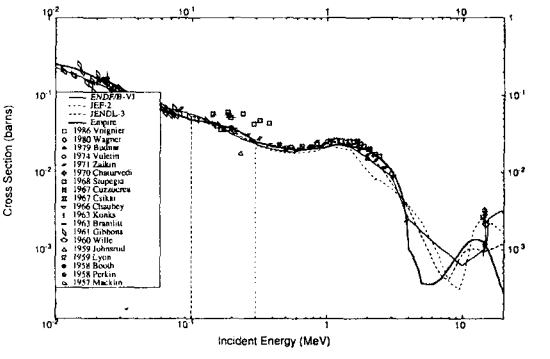

Fig. 3. Capture Cross Section for Pr-141

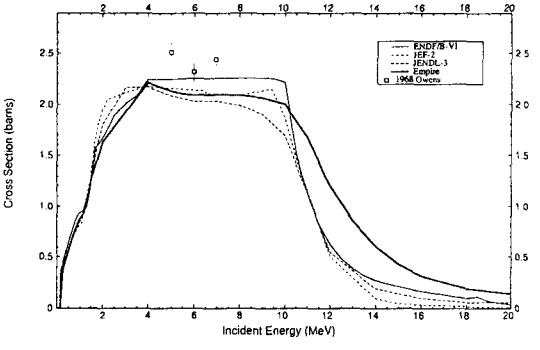

Fig. 2. (n, n') Cross Section for Pr-141

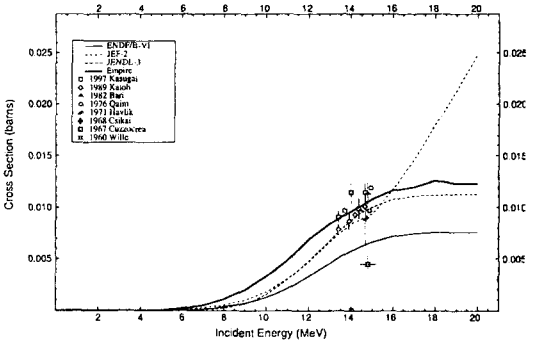

Fig. 4. (n, p) Cross Section for Pr-141

function value was referenced from the evaluation of resonance parameters. Fig. 2 shows the (n, n') cross section. The enhanced (n, n') cross section calculation in the higher energy region by multistep direct reaction was given. Fig. 3 shows the (n, γ) cross section results. The calculation follows the experimental data[13,17] very well and shows the direct capture contribution by the de-excitation of GDR around 14 MeV. There is good agreement for capture cross section between ENDF/B-VI and calculation in the measurement energy range. Fig. 4 is for the (n, p) cross section. The calculated result is in good agreement with the experimental data[14]. The ENDF/B-VI is lower than the reference experimental data and the calculation. Fig. 5 is for the (n, α) cross section results. There is one old piece of experimental data at 14.7 MeV. Even though the calculation has agreement with the data within fluctuation at that energy point, the conclusion can not be made here.

Fig. 6 shows the calculated total cross section with the experimental data[15] and the evaluated files for Nd-143. The model calculation follows the reference experimental data well. There is difference slightly between the calculation and ENDF/B-VI in higher energy area. Fig. 7 shows the (n, n') cross section. There is no experimental data. Fig. 8 shows the capture cross section. Above 80 keV, there is much difference between the calculation and the ENDF/B-VI. However, in the measurement energy range, the calculation is

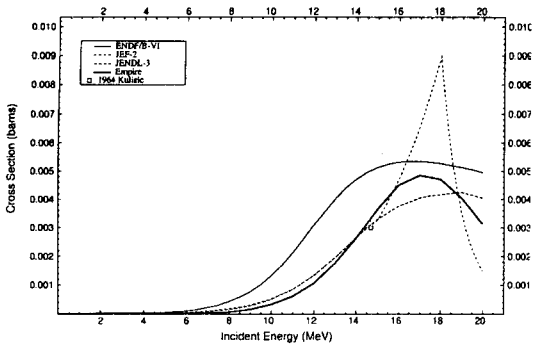

Fig. 5. (n, α) Cross Section for Pr-141

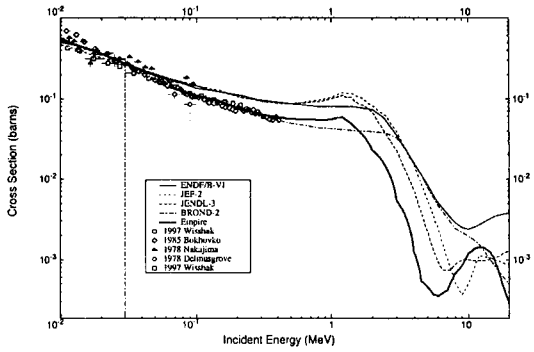

Fig. 8. Capture Cross Section for Nd-143

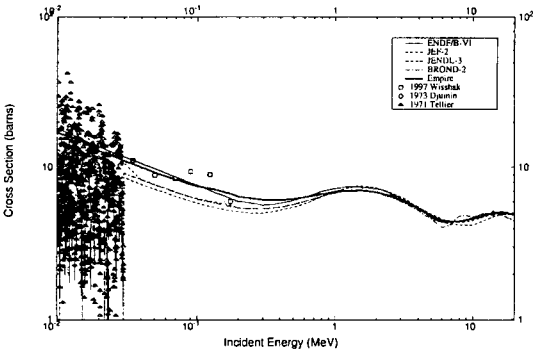

Fig. 6. Total Cross Section for Nd-143

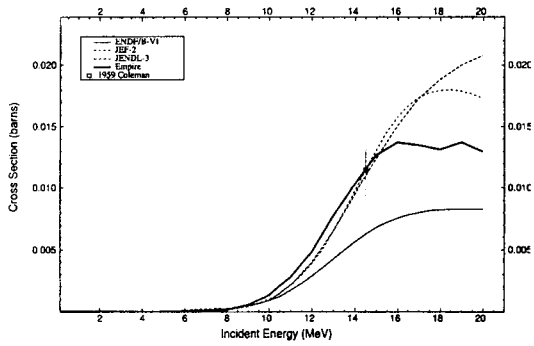

Fig. 9. (n, p) Cross Section for Nd-143

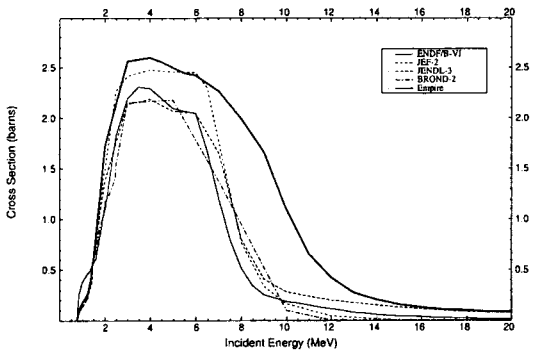

Fig. 7. (n, n') Cross Section for Nd-143

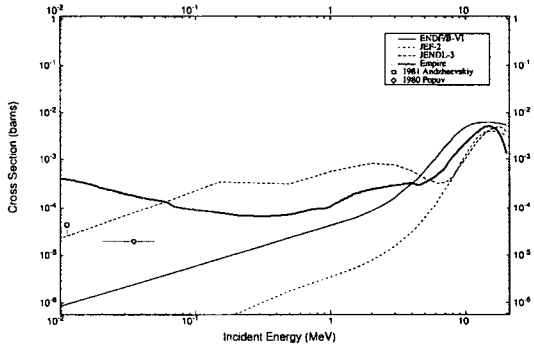

Fig. 10. (n, α) Cross Section for Nd-143

in good agreement with the experimental data[15,18,19]. Fig. 9 is (n, p) cross section and Fig. 10 is for (n, α) cross section.

The calculated total cross section for Nd-145 is compared with the experimental data in Fig. 11. In the measured area, ENDF/B-VI is a little higher than the calculation and measured data. The calculated total cross section follows the reference

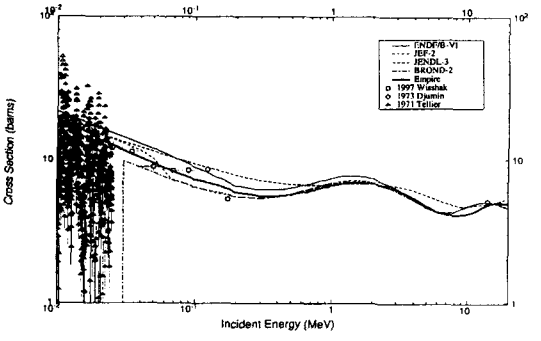

Fig. 11. Total Cross Section for Nd-145

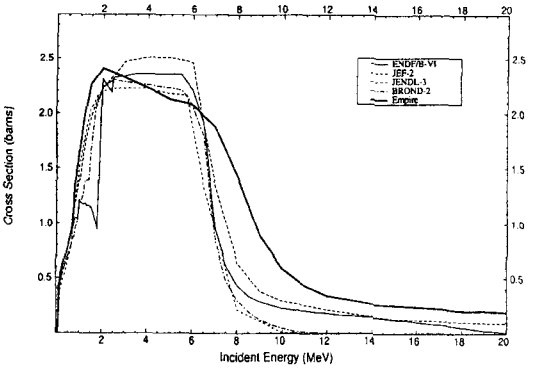

Fig. 12. (n, n') Cross Section for Nd-145

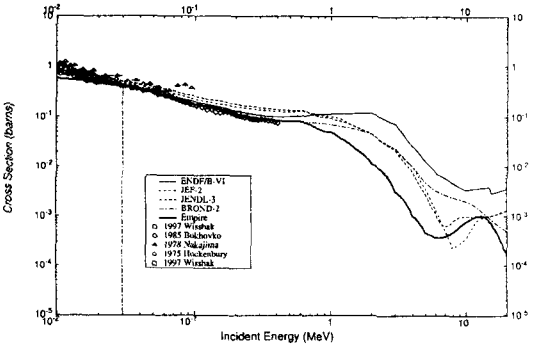

Fig. 13. Capture Cross Section for Nd-145

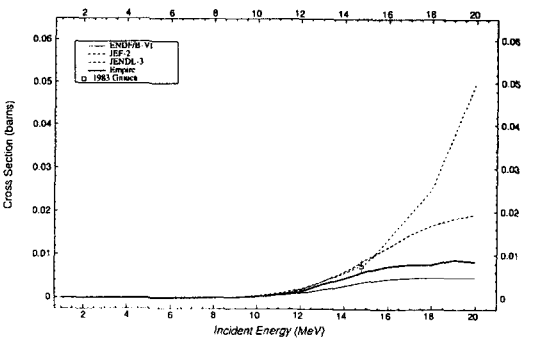

Fig. 14. (n, p) Cross Section for Nd-145

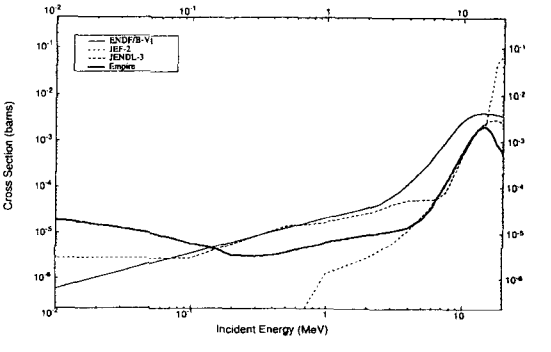

Fig. 15. (n, α) Cross Section for Nd-145

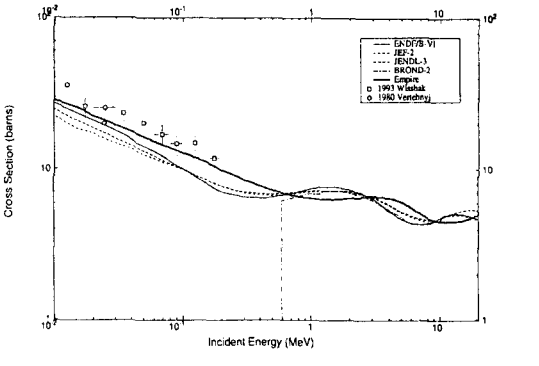

Fig. 16. Total Cross Section for Sm-147

experimental data[15] well. Fig. 12 is the (n, n') cross section. Fig. 13 shows the calculated, the measured and the ENDF/B-VI capture cross sections. The calculated capture cross section is in good agreement with the reference experimental data[15] above 20 keV. The calculated capture cross section in the lower energy region might be substituted by the resonance parameters[2]. Above 60 keV, the different capture cross section starts between the calculation and the ENDF/B-VI. Fig.

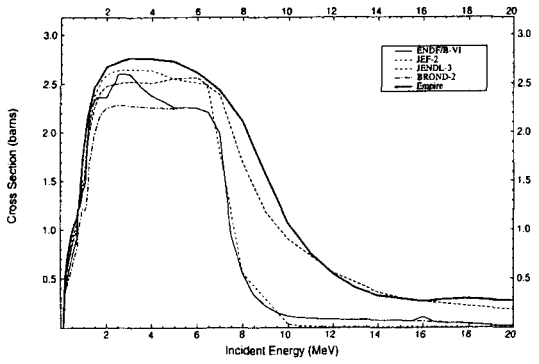

Fig. 17. (n, n') Cross Section for Sm-147

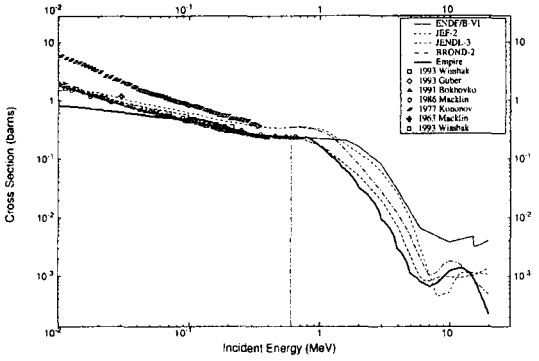

Fig. 18. Capture Cross Section for Sm-147

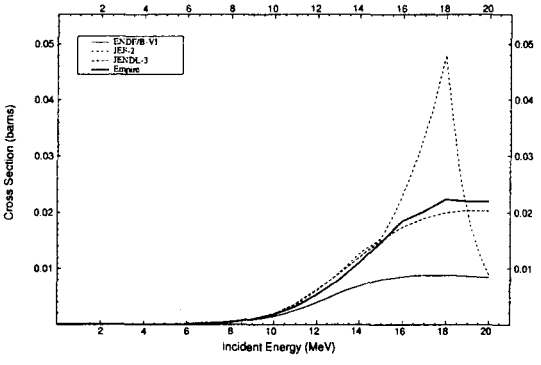

Fig. 19. (n, p) Cross Section for Sm-147

14 shows (n, p) cross section. Within fluctuation error, there is an agreement with the experimental data at 14.7 MeV. Fig. 15 is (n, α) cross section data.

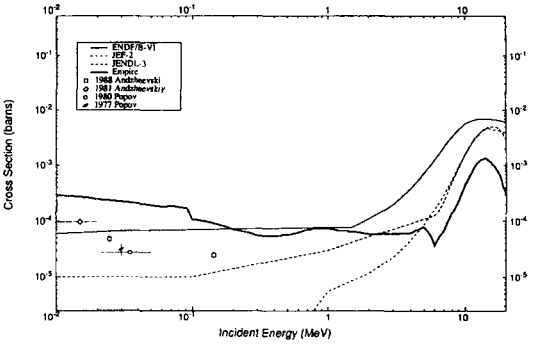

Fig. 20. (n, α) Cross Section for Sm-147

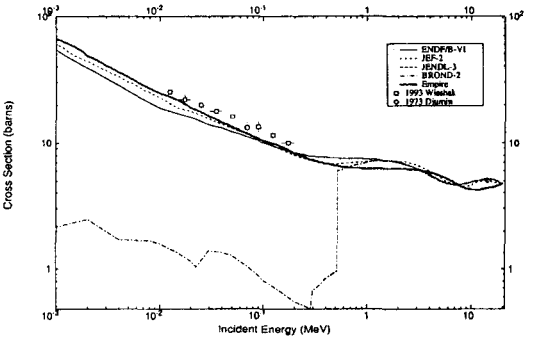

Fig. 21. Total Cross Section for Sm-149

Fig. 16 shows the total cross section of Sm-147. The calculation is in good agreement with the measured data[16]. However, the calculation is different from the ENDF/B-VI. At low energy, the s-wave strength function value was referenced from the evaluation of resonance parameters. Fig. 17 is (n, n') cross section. Fig. 18 shows the capture cross section. Model calculation shows a poor capture cross section to the measured data below 60 keV, On the other hand, ENDF/B-VI follows the experimental data up to 800 keV. However, above 800 keV, the current calculation is much different from the ENDF/B-VI. The resonance parameters will cover up to 1st excited energy. From 100 to 200 keV, the calculation follows the Wisshak[16] data and ENDF/B-VI does

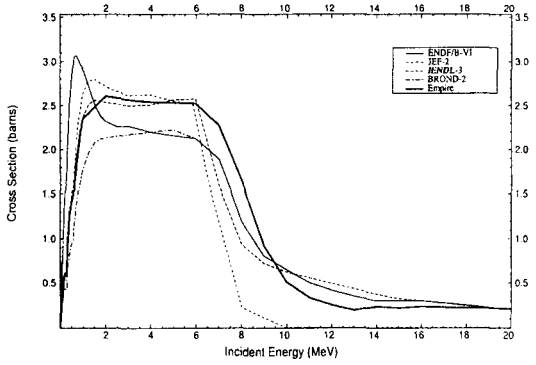

Fig. 22. (n, n') Cross Section for Sm-149

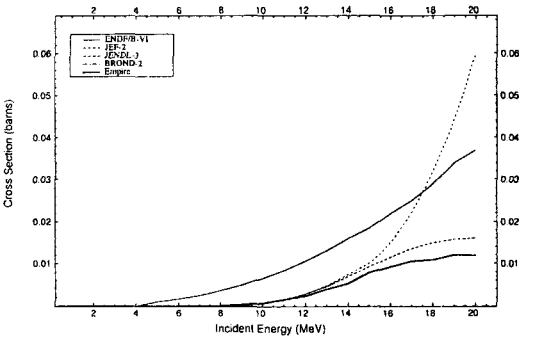

Fig. 24. (n, p) Cross Section for Sm-149

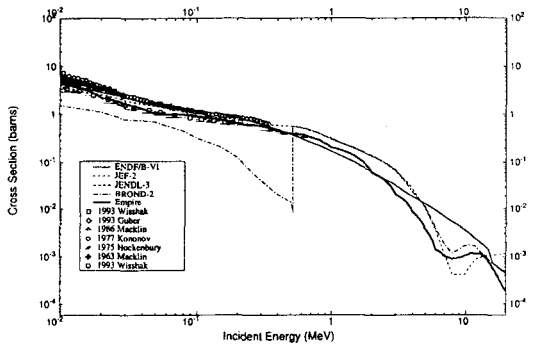

Fig. 23. Capture Cross Section for Sm-149

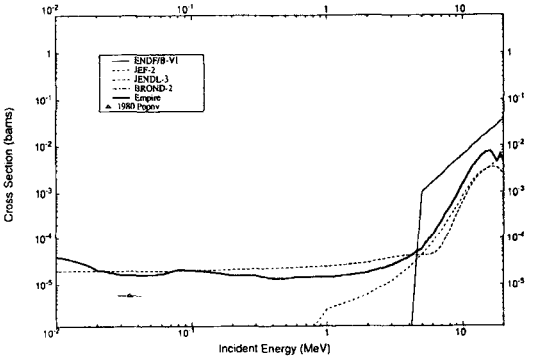

Fig. 25. (n, α) cross section for Sm-149

Macklin[20] data. Fig. 19 is (n, p) cross section. There is no experimental data. Fig. 20 is (n, α) cross section.

The model calculated total cross section of Sm-149 follows the reference experimental data[16] well than ENDF/B-VI in Fig. 21. Fig. 22 is (n, n') cross section. Fig. 23 shows the capture cross section. There is no much difference between the current evaluation and the ENDF/B-VI in the measured energy range. The current calculation follows the Wisshak data[16] and ENDF/B-VI follows the Kononov data[21]. Fig. 24 and 25 are (n, p) and (n, α) cross sections.

The elastic and other threshold reaction cross sections are not shown here, but the results were summarized in ENDF-6 formatted files. In this paper, the evaluation started from 10 keV, around which major experiment data existed and the final results will be merged with the evaluation for resonance part at the 1st excited energy.

4. Conclusions

The selected energy dependent optical model potential was proper to produce the model calculated cross sections in the evaluation energy range. The s-wave strength function was helpful in obtaining the total cross section closer to the experimental data. Empire was successful in producing the reaction cross sections. Width fluctuation correction was functioned in the (n, γ) and (n, n') cross sections in equilibrium energy

region and the (n, γ) and (n, p) cross sections in the pre-equilibrium energy region were enhanced in the new Empire version. Evaluated cross sections were in good agreement with the experimental data and enhanced the ENDF/B-VI. However, evaluated capture cross section for Sm-147 was exceptional until 60 keV. In this case, resonance parameters will cover that energy range. The results will be submitted in the ENDF/B-VI to improve neutron data.

Acknowledgements

This work is performed under the auspices of Korea Ministry of Science and Technology as a long-term R&D project.

References

1. J.H. Chang et al., Establishment of Nucelar Data System, KAERI/RR-2121/(2000).
2. S.Y.Oh and J.H.Chang, Neutron Cross Section Evaluations of Fission Products below the Fast Energy Region, BNL-NCS-67469 (KAERI/TR-1511/2000), Brookhaven Natoinal Laboratory.
3. Y. D. Lee, "ABRXPL development for parameter decision of spherical optical model potential," KAERI, NDL-14/99.
4. R.D.Lawson, ABAREX_A Neutron Spherical Optical-Statistical Model Code, in Workshop on Computation and Analysis of Nuclear Data Relevant to Nuclear Energy and Safety, pp447, Trieste, Italy.
5. M.Herman, Empire-II: Statistical Model Code for Nuclear Reaction Calculations, IAEA, (2000).
6. S. Igarasi, Optical Model Potentials used in JENDL Evaluations (JAERI, Tokaimura, Japan), Reference Input Parameter Library for theoretical calculations of nuclear reactions (RIPL), JAERI 1228(41), (1973).
7. T. Nakagawa, et al., Japanese Evaluated Nuclear Data Library, Version 3, Revision 2, J. Nucl. Sci. Technol. 32, 1259, (1995).
8. T. Tamura, T. Udagawa and H. Lenske, Phys. Rev. C26, 379, (1982).
9. H. Nishiok, J.J.M. Verbaarschot, H.A. Weidenmuller and S. Yoshida, Ann. Phys. 172, 67, (1986).
10. R. Singh, H.H. Knitter, "Measurement of Fast Neutron Scattering and Total Cross Sections of 141-Pr," J, ZP/A, 272, 47, (1975).
11. J.D. Kellie, The Neutron Total Cross Sections of Some Rare Earth Elements Between 0.7 MeV and 9.0 MeV," J, JP/A, 7, 1758, 1974.
12. D.G. Foster, JR,D.W. Glasgow, "Neutron Total Cross Sections, 2.5 - 15 MeV.," J, PR/C, 3, 576, (1971).
13. G.G. Zaikin et al., "Radiative Capture Cross-Sections of Fast Neutrons by Ga-69, Ga-71, La-139 and Pr-141 Isotopes," J, UFZ, 16,(7), 1205, (1971).
14. Y. Kasugai, Y. Ikeda and Y. Uno, "Activation Cross Section Measurement for La, Ce, Pr, Nd, Gd, Dy and Er Isotopes by 14 MeV Neutrons," C, 97Trieste, 1, 635, (1997).
15. K. Wisshak, "Stellar neutron capture cross section of the Nd isotopes," Physical Review C, Vol. 57, No. 1, pp391-407, Jan. (1998).
16. K. Wisshak, "Neutron Capture in 148, 150Sm: A sensitive Probe of the s-probe neutron density," Physical Review C, Vol. 48, No. 3, pp1401-1419, Sept. (1993).
17. J. Voignier, S. Joly, G.Grenier, "Capture Cross Sections and Gamma-Ray Spectra from the Interaction of 0.5 to 3.0 MeV Neutron with Nuclei in the Mass Range A=63 to 209," J, NSE, 93, 43, (1986).
18. M. V. Bokhovko, "Radiative capture cross-section measurement for Nd-143 and -145 isotopes in the energy range 4-420keV," Vopr. At. Nauki I Tekhn., Ser. Jad. Konst.,

Vol.3, pp12, (1985).
19. R. W. Hockenbury, "Capture Cross sections of 145-Nd, 149-Sm, 101-Ru, 102-Ru, and 104-Ru," Bull. Amer. Phys. Soc., Vol.20, pp560, (1975).
20. R. Macklin, EXFOR12966, ORNL, (1986).
21. V. N. Kononov, "Average Neutron Radiation Capture Cross-section in the Energy Range 5-30 keV for In, Ta, Au, Nd, Sm, Eu, Gd, Er Isotopes," Report of Nucl. Const, YK-22, (1977).
22. Y.D. Lee and J.H. Chang, "Evalustion of Neutron Cross Section for Nd-143, Nd-145, Sm-147 and Sm-149 from 1 keV to 20 MeV," Korean Nuclear Society Autumn Meeting, Oct. 26, (2001).